Korean J Physiol Pharmacol 2016;20(3):315-324
http://dx.doi.org/10.4196/kjpp.2016.20.3.315

KJPP

Original Article

Effects of hydrogen peroxide on voltage-dependent K^+ currents in human cardiac fibroblasts through protein kinase pathways

Hyemi Bae[1], Donghee Lee[1], Young-Won Kim[1], Jeongyoon Choi[1], Hong Jun Lee[2], Sang-Wook Kim[3], Taeho Kim[3], Yun-Hee Noh[4], Jae-Hong Ko[1], Hyoweon Bang[1], and Inja Lim[1,*]

[1]*Department of Physiology,* [2]*Biomedical Research Institute,* [3]*Department of Internal Medicine, College of Medicine, Chung-Ang University, Seoul 06974,* [4]*Department of Biochemistry, School of Medicine, Konkuk University, Seoul 05029, Korea*

ARTICLE INFO

Received March 8, 2016
Revised April 1, 2016
Accepted April 4, 2016

***Correspondence**
Inja Lim
E-mail: injalim@cau.ac.kr

Key Words
Ca^{2+}-activated K^+ channels
Human cardiac fibroblasts
Hydrogen peroxide
K^+ currents
Protein kinase

ABSTRACT Human cardiac fibroblasts (HCFs) have various voltage-dependent K^+ channels (VDKCs) that can induce apoptosis. Hydrogen peroxide (H_2O_2) modulates VDKCs and induces oxidative stress, which is the main contributor to cardiac injury and cardiac remodeling. We investigated whether H_2O_2 could modulate VDKCs in HCFs and induce cell injury through this process. In whole-cell mode patch-clamp recordings, application of H_2O_2 stimulated Ca^{2+}-activated K^+ (K_{Ca}) currents but not delayed rectifier K^+ or transient outward K^+ currents, all of which are VDKCs. H_2O_2-stimulated K_{Ca} currents were blocked by iberiotoxin (IbTX, a large conductance K_{Ca} blocker). The H_2O_2-stimulating effect on large-conductance K_{Ca} (BK_{Ca}) currents was also blocked by KT5823 (a protein kinase G inhibitor) and 1 H-[1, 2, 4] oxadiazolo-[4, 3-a] quinoxalin-1-one (ODQ, a soluble guanylate cyclase inhibitor). In addition, 8-bromo-cyclic guanosine 3′, 5′-monophosphate (8-Br-cGMP) stimulated BK_{Ca} currents. In contrast, KT5720 and H-89 (protein kinase A inhibitors) did not block the H_2O_2-stimulating effect on BK_{Ca} currents. Using RT-PCR and western blot analysis, three subtypes of K_{Ca} channels were detected in HCFs: BK_{Ca} channels, small-conductance K_{Ca} (SK_{Ca}) channels, and intermediate-conductance K_{Ca} (IK_{Ca}) channels. In the annexin V/propidium iodide assay, apoptotic changes in HCFs increased in response to H_2O_2, but IbTX decreased H_2O_2-induced apoptosis. These data suggest that among the VDKCs of HCFs, H_2O_2 only enhances BK_{Ca} currents through the protein kinase G pathway but not the protein kinase A pathway, and is involved in cell injury through BK_{Ca} channels.

INTRODUCTION

Cardiac fibroblasts (CFs) are the largest population of cells in the heart, and they play a critical role in maintaining its normal function and homeostasis [1]. These cells contribute to the structural, biochemical, mechanical, and electrical characteristics of the heart and are the main source of collagen, which is the most important component of the cardiac extracellular matrix [2]. Excessive extracellular matrix deposition and CFs proliferation lead to heart failure, sudden cardiac death, and other serious complications [3]; therefore, these cells act as mediators of inflammatory and fibrotic myocardial remodeling in injured hearts [4,5].

It has been reported that extensive networks exist between CFs and cardiomyocytes through numerous anatomical contacts, which suggests potential heterocellular electrical coupling in diseased myocardium in arrhythmogenesis [2,6,7].

The ion channels present in cardiomyocytes and their functions

Author contributions: H.B., D.L., Y.K., and J.C. performed experiments. H.B., I.L., J.K., and H.B. analyzed and interpreted data. H.B. and I.L. wrote the manuscript. H.J.L., S.K., T.K., Y.N. and H.B. revised the manuscript. I.L. supervised and coordinated the study.

have been well studied. CFs also have multiple ion channels, but their distribution and properties are quite distinct from those in cardiomyocytes [8]. It is well known that K^+ channel-mediated signals, especially from voltage-dependent K^+ channels (VDKCs), play an important role in cell death or apoptosis in many cell types [9-13]. There are two types of VDKCs, Ca^{2+}-activated K^+ (K_{Ca}) channels and voltage-gated K^+ (K_V) channels. These channels are found in nearly every cell type, which suggests their physiological importance.

K_{Ca} channels can regulate membrane potential and intracellular K^+ concentration, and constitute a major link between second messengers and the electrical activity of cells. There are three families of K_{Ca} channels that are based on differences in their biophysical and pharmacological properties, large-conductance K_{Ca} (BK_{Ca} or $K_{Ca}1.1$), intermediate-conductance K_{Ca} (IK_{Ca} or $K_{Ca}3.1$), and small-conductance K_{Ca} (SK_{Ca} or $K_{Ca}2.x$) channels. The ubiquitous BK_{Ca} channels are composed of pore-forming α subunits and four auxiliary β subunits, and gating is regulated by Ca^{2+} and membrane voltage [14]. BK_{Ca} currents have large conductances of 100~250 and 200~300 pS in physiological K^+ gradients and a symmetrical 140 mM K^+ solution, respectively [15]. In contrast, IK_{Ca} channels are voltage-independent and have intermediate single channel conductance values of 20~80 pS in physiological conditions [16]. Finally, SK_{Ca} channels have a small unitary conductance of 4~14 pS [17].

Kv channels modulate electrical excitability, regulate the repolarization of action potential, and are divided into two subfamilies, delayed rectifier K^+ (K_{DR}) or transient outward K^+ (K_{TO}). K_{DR} channels show fast activating kinetics with slow inactivation or no inactivation, whereas K_{TO} channels show fast activation and inactivation kinetics [18,19].

Hydrogen peroxide (H_2O_2), an oxidative stress inducer, is the main contributor to cardiac injury and remodeling [20]. H_2O_2 has been shown to activate or inhibit ion channels depending on channel type; it inhibits voltage-gated K_{TO} currents and K_{DR} currents in rat hippocampal neurons [21], but enhances BK_{Ca} currents in human dermal fibroblasts [9] and human endothelial cells through the cGMP signaling pathway [22]. In cardiomyocytes, H_2O_2 decreased K_{DR} currents in the ventricular myocytes of adult guinea pigs and increased apoptosis [23]. In contrast, H_2O_2 decreased K_{TO} currents but increased K_{DR} currents in rabbit atrial myocytes [24]. However, in human CFs (HCFs), whether H_2O_2 can modulate K^+ channels and its mechanism still remain unclear.

In this study, we identified three types of VDKCs in HCFs and investigated the effects of H_2O_2 on these K^+ channels using a whole-cell patch-clamp technique. The key protein kinase pathways involved in the observed effects of H_2O_2 on the K^+ currents and H_2O_2-induced injury of HCFs as well as the relationship between H_2O_2-induced injury and K^+ currents were also investigated.

METHODS

Cell preparation and culture

Human cardiac fibroblasts (adult ventricle, Catalog #6310) were purchased from ScienCell Research Laboratory (San Diego, CA). Cells were cultured in Dulbecco's modified Eagle's medium (DMEM; Welgene, Korea) supplemented with 10% fetal bovine serum (FBS; Welgene) and penicillin-streptomycin solution (GenDEPOT, Barker, TX) in a humidified atmosphere of 5% CO_2 and 95% air at 37°C. Confluent fibroblasts were detached by incubation with 0.25% trypsin (Welgene) and DMEM for a few minutes. The detached cells were pelleted by centrifugation, the supernatant was removed, and the pellet was suspended in 1 mL of bath solution. Cells used in this study were from early passages (3 to 7) to limit possible variation.

Electrophysiological recordings

A small aliquot of solution containing HCFs was placed in an open perfusion chamber mounted on the stage of an inverted microscope. Whole-cell currents were recorded with an Axopatch 200B patch clamp amplifier (Axon Instruments, Union City, CA) at room temperature. pCLAMP 9.0 software (Axon Instruments) was used for data acquisition and analysis of whole-cell currents. Activated currents were filtered at 2 kHz and digitized at 10 kHz. Patch pipettes were prepared from filament-containing borosilicate tubes (TW150F-4; World Precision Instruments, Sarasota, FL) using a two-stage microelectrode puller (PC-10; Narishige, Tokyo, Japan), and then fire polished on a microforge (MF-830; Narishige). When filled with pipette solution, the pipettes exhibited a resistance of 2~3 MΩ. The bath solution used for whole-cell recordings contained (in mM): 145 NaCl, 5 KCl, 1 $CaCl_2$, 1 $MgCl_2$, 5 glucose, and 5 HEPES (pH adjusted to 7.35 with NaOH). The pipette solution for patch clamping contained (in mM): 145 KCl, 1.652 $CaCl_2$ (pCa 6.0), 1.013 $MgCl_2$, 10 HEPES, 2 EGTA, and 2 K-ATP (pH adjusted to 7.3 with KOH). H_2O_2, iberiotoxin (IbTX, a BK_{Ca} channel blocker), KT5823 (a protein kinase G inhibitor), 1H-[1,2,4]-oxadiazolo [4,3-a]quinoxalin-1-one (ODQ, a soluble guanylyl cyclase inhibitor), 8-bromo-cyclic guanosine 3', 5'-monophosphate (8-Br-cGMP), KT5720 and H-89 (protein kinase A inhibitors), and all other chemicals were purchased from Sigma-Aldrich (St. Louis, MO).

Reverse transcription polymerase chain reaction (RT-PCR)

Total RNA was extracted from HCFs using the Total RNA Isolation PureLink RNA Mini Kit (Ambion, Carlsbad, CA). First-strand cDNA was prepared with the SuperScript III Cells Direct cDNA Synthesis Kit (Invitrogen, Tokyo, Japan). Reverse transcription was performed in a S1000 Thermal Cycler (Bio-Rad,

Hercules, CA), according to the manufacturer's instructions. RT-PCR reaction products (cDNA) were resolved by 1.2% agarose gel electrophoresis, and stained with ethidium bromide for visualization under ultraviolet light. The primer sequences are listed in Table 1.

Western blot analysis

The cells were rinsed twice with ice-cold phosphate buffered saline (PBS) and then lysed in ice-cold lysis buffer. After incubation on ice for 30 min with shaking, the samples were centrifuged at 14,000 rpm for 10 min at 4°C. The protein concentration was measured by the Bradford assay. Extracts containing 20 μg of protein were mixed with 5× sample buffer, boiled for 10 min, and then subjected to continuous electrophoresis using 10~12% SDS-PAGE gels. The separated proteins were transferred to polyvinylidene difluoride (PVDF) membranes (IPVH00010; EMD Millipore, Billerica, MA) by electrophoretic transfer and blocked with 5% skim milk in tris-buffered saline containing 0.1% Tween-20 (TBS-T) for 1 h at room temperature. The membranes were rinsed and incubated with primary antibodies at 4°C overnight. Removal of primary antibodies was carried out by washing for 4×10 min in TBS-T. The secondary antibodies were incubated with membrane in TBS-T with 5% skim milk for 1 h at room temperature. After a final wash with TBS-T for 4×15 min, the bands were detected using the chemiluminescence system (ECL, Thermo Fisher Scientific, Rockford, IL). The results were analyzed with Bio-Rad molecular analysis software. The primary and secondary antibodies used are listen in Table 2.

Annexin V/propidium iodide apoptosis assay

Apoptosis of HCFs was determined using flow cytometric analysis. Cellular apoptosis was observed by annexin V-FITC/PI double staining using the Annexin V/Dead Cell Apoptosis Kit (Invitrogen) according to the manufacturer's instructions. Briefly, cells were seeded at a density of 6×10^5 cells/mL and cultured in DMEM containing 100 μM H_2O_2 for 6 h, or with IbTX for 24 h, and then 100 μM H_2O_2 was added and incubated for 6 h. Cells were harvested by treatment with trypsin, and then washed twice with cold PBS and centrifuged to collect the cell pellet. Annexin V-FITC and PI were added, and the cells were incubated in the dark at room temperature. Cells were analyzed with a flow cytometer (BD Biosciences) at 530 nm. Data from 10,000 cells were collected for each data file. Annexin V-FITC-positive and PI-negative cells were defined as apoptotic cells. Finally, the number of cells in each category was expressed as a percentage of the total number of stained cells.

Statistical analysis

Data are expressed as the mean±standard error of the mean (S.E.M.). Comparison of measurements between groups was performed using Student's t-test or one way ANOVA, depending on the experimental design. Differences were considered sig-

Table 1. Primers used for RT-PCR

Gene		Sequence	Size, bp
GAPDH	Forward	5′-AGCCACATCGCTCAGACACC-3′	302
	Reverse	5′-GTACTCAGCGGCCAGCATCG-3′	
$K_{Ca}1.1\alpha$	Forward	5′-CTACTGGGATGTTTCACTGGTGT-3′	444
	Reverse	5′-TGCTGTCATCAAACTGCATA-3′	
$K_{Ca}1.1\beta1$	Forward	5′-TCTACTGCTTCTCCGCAC-3′	363
	Reverse	5′-GAGCAGGCAATGACTTCA-3′	
$K_{Ca}1.1\beta2$	Forward	5′-GGGACTGGCTATGATGGT-3′	449
	Reverse	5′-GTGAATGGAACAGCACGTTG-3′	
$K_{Ca}1.1\beta3$	Forward	5′-GCTCAACAGTGCTCTGGACA-3′	351
	Reverse	5′-TGGCCACCGTCTTAAGATTT-3′	
$K_{Ca}1.1\beta4$	Forward	5′-CTGAGTCCAACTCTAGGGCG-3′	300
	Reverse	5′-TGGTCAGGACCACAATGAGA-3′	
$K_{Ca}2.1$	Forward	5′-TGGACACTCAGCTCACCAAG-3′	208
	Reverse	5′-TTAGCCTGGTCGTTCAGCTT-3′	
$K_{Ca}2.2$	Forward	5′-GCGTCGCTGTATTCCTTAGC-3′	334
	Reverse	5′-GCATGACTCTGGCAATCAGA-3′	
$K_{Ca}2.3$	Forward	5′-ACCCCCTCTTCTTTCTCCAA-3′	173
	Reverse	5′-CTCAAAGAAAGCCAGGCATC-3′	
$K_{Ca}3.1$	Forward	5′-GAGAGGCAGGCTGTTAATGC-3′	215
	Reverse	5′-ACGTGCTTCTCTGCCTTGTT-3′	

$K_{Ca}1.1$, large conductance type of K_{Ca} (BK_{Ca}) channels; $K_{Ca}2.1$~2.3, small conductance type of K_{Ca} channel ($SK_{Ca}1$~3); $K_{Ca}3.1$, intermediate conductance type of K_{Ca} (IK_{Ca}) channel.

Table 2. List of primary and secondary antibodies

Primary Antibody	Species	Catalog No.	Dilution	KDa	Company
Beta-Actin	Mouse monoclonal	ab6276	1:5000	42	Abcam
Maxi Kα	Goat polyclonal	sc-14746	1:200	125	Santa Cruz
Maxi Kβ	Goat polyclonal	sc-14751	1:200	22	Santa Cruz
KCNN2	Rabbit polyclonal	ab83733	1:300	64	Abcam
KCNN3	Rabbit polyclonal	ab28631	2 μg/ml	82	Abcam
KCNN4	Rabbit polyclonal	ab83740	1:300	47	Abcam
Secondary Antibody					
Donkey anti-goat IgG-HRP		sc-2020	1:2000		Santa Cruz
Amersham ECL Anti-Rabbit IgG, HRP-linked Whole Antibody (from donkey)		NA934	1:5000		GE Healthcare
Amersham ECL Anti-Mouse IgG, HRP-linked Whole Antibody (from sheep)		NA931	1:2000		GE Healthcare

Maxi K, large conductance calcium-activated potassium channels ($K_{Ca}1.1$, BK_{Ca}); KCNN2, small conductance calcium-activated potassium channels ($K_{Ca}2.2$, $SK_{Ca}2$); KCNN3, small conductance calcium-activated potassium channels ($K_{Ca}2.3$, $SK_{Ca}3$); KCNN4, intermediate conductance calcium-activated potassium channels ($K_{Ca}3.1$, IK_{Ca}).

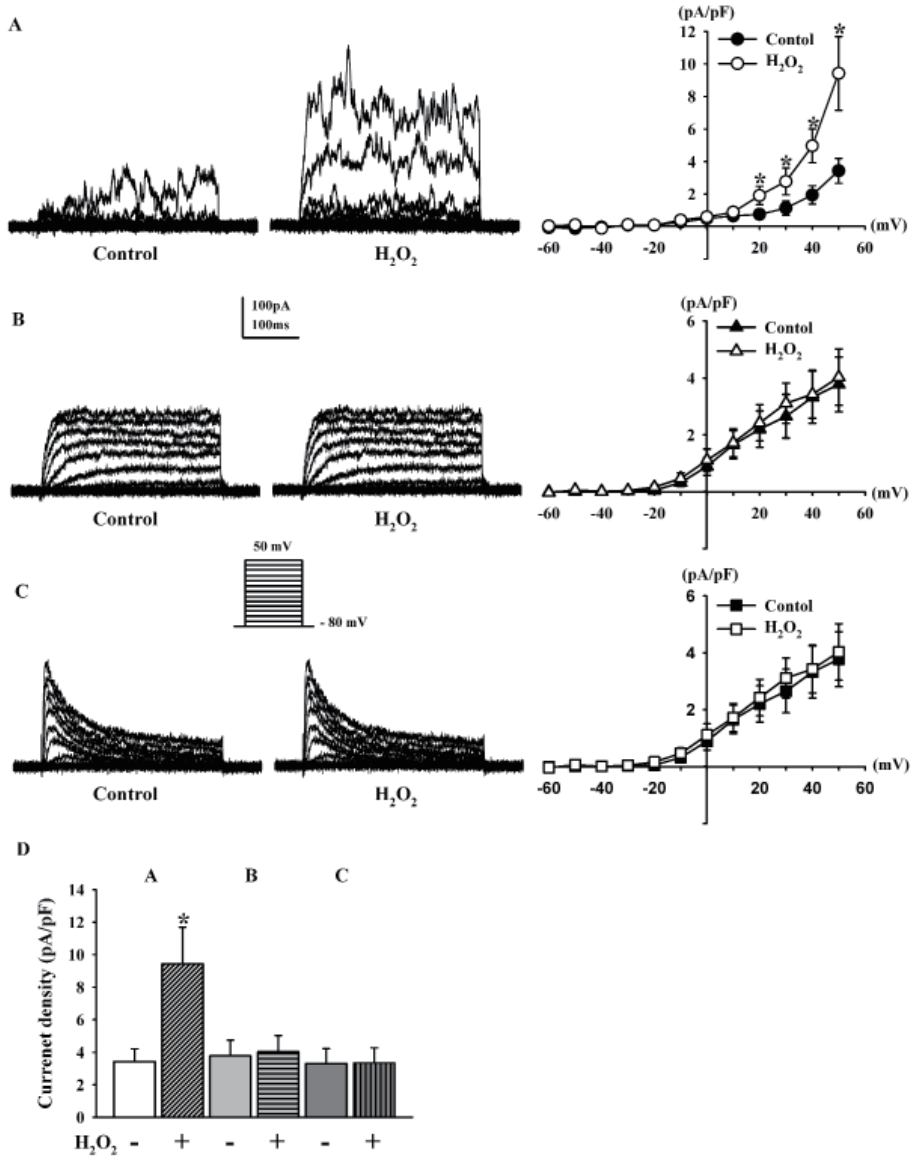

Fig. 1. Identification of outward K^+ currents in human cardiac fibroblasts and effect of H_2O_2. Representative K^+ current traces were obtained by voltage step pulses from −80 mV to +50 mV for 400 ms in whole-cell mode patch clamp recordings (holding potential, −80 mV). (A) Strongly oscillating, non-inactivating K_{Ca} currents are stimulated by H_2O_2. (B) Fast activation with slow or non-inactivation K_{DR} currents are not stimulated by H_2O_2. (C) Fast activating with rapid inactivation K_{TO} currents are not stimulated by H_2O_2. (D) Current densities of K_{Ca} currents, K_{DR} currents, and K_{TO} currents, at +50 mV from a holding potential of −80 mV, in control cells and after the addition of H_2O_2. *p<0.05, versus the control.

 http://dx.doi.org/10.4196/kjpp.2016.20.3.315

nificant at p values less than either 0.05 or 0.01.

RESULTS

Identification of outward K^+ currents and effect of H_2O_2 in human cardiac fibroblasts

Macroscopic K^+ currents were generated using a voltage protocol that consisted of depolarizing steps (from −80 mV to +50 mV) in 10 mV increments for 400 ms with a −80 mV holding potential in whole-cell mode patch-clamp recordings. Ca^{2+}-activated K^+ (K_{Ca}) channels and voltage-gated K^+ (K_V) currents with typical behavior were recorded in HCFs. K_{Ca} currents showed strong oscillation in response to strong depolarization, were well maintained throughout the test pulse without marked inactivation during depolarizing voltage increments, and their current-voltage (I~V) relationship showed strong outward rectification (Fig. 1A). These currents were detected in 47% (197 out of 419) of cells. Two types of K_V currents could be distinguished based on their activation and inactivation kinetics: fast activating and slow or non-inactivating currents, called delayed rectifier K^+ (K_{DR}) currents (Fig. 1B), and fast activating and inactivating currents, called transient outward K^+ (K_{TO}) currents (Fig. 1C). K_{DR} and K_{TO} currents were detected in 46.8% and 6.2% of cells, respectively. They did not show the outward rectification in their I~V curves.

To determine the effect of H_2O_2 on outward K^+ currents in HCFs, H_2O_2 (100 μM) was added to the bath solution. In the presence of H_2O_2, K_{Ca} currents were significantly increased (Fig. 1A). This increase was 274.6±29.7% of that in the absence of H_2O_2 at +50 mV (n=13, *p<0.05 vs. control). The current densities of K_{Ca} currents at +50 mV in the absence and presence of H_2O_2 were 3.43±0.77 pA/pF and 9.42±2.27 pA/pF, respectively (n=13, p<0.05, Fig. 1D). In contrast, H_2O_2 had no significant effects on K_{DR} currents (106.7±10.3% of the control, n=12, Fig. 1B) or K_{TO} currents (101.2±10.1% of the control, n=8; Fig. 1C). At +50 mV, the current densities did not differ (control K_{DR}, 3.77±0.96 pA/pF vs. with H_2O_2, 4.03±0.99 pA/pF; control K_{TO}, 3.30±0.91 pA/pF vs. with H_2O_2, 3.34±0.92 pA/pF, Fig. 1D)

Identification of K_{Ca} channels in human cardiac fibroblasts

To determine which of the K_{Ca} channels subtypes are present in HCFs, K_{Ca} channel gene expression was examined by RT-PCR using specific primers for the K_{Ca} channel families (shown in Table 1). We detected clear amplification of the mRNA encoding the pore-forming α subunit of the $K_{Ca}1.1(BK_{Ca})$ channel along with the auxiliary 1.1β1, 1.1β3, and 1.1β4 subunits (Fig. 2A). The mRNA expression of the $K_{Ca}2.2$ and $K_{Ca}2.3$ subunits of the SK_{Ca} channel and the $K_{Ca}3.1$ subunit of the IK_{Ca} channel was also detected by RT-PCR. Expression of the $K_{Ca}1.1β2$ subunit of BK_{Ca} and the $K_{Ca}2.1$ subunit of SK_{Ca} was not detected. To examine whether the ion channels that were detected by RT-PCR were expressed in protein form, a western blot analysis was performed. As shown in Fig. 2B, the expected sizes of immunoreactive protein bands for the BK_{Ca} channel subunits ($K_{Ca}1.1α$ and $K_{Ca}1.1β$) were detected (molecular weights, 125 kDa and 22 kDa, respectively). Expression of the subunits of the SK_{Ca} channels $K_{Ca}2.2$ and $K_{Ca}2.3$ and the IK_{Ca} channel $K_{Ca}3.1$ was also detected as prominent bands of molecular weights 64 kDa, 82 kDa, and 47 kDa, respectively. β-Actin (42 kDa) was used as a control for normalization.

Identification of BK_{Ca} channels and their role in H_2O_2-induced apoptosis in human cardiac fibroblasts

Previous studies have suggested that BK_{Ca} channels are the predominant K_{Ca} channels in HCFs [8,9,25]. Here, we employed IbTX, a specific BK_{Ca} channel blocker, to examine whether the K^+ currents modulated by H_2O_2 were BK_{Ca} currents. IbTX (100 nM) significantly inhibited the strong oscillation of K_{Ca} currents (44.2±7.4% of the control at 50 mV, n=6, *p<0.05 vs. control; Fig. 3A). The current densities of K_{Ca} currents at +50 mV in the absence and presence of IbTX were 3.38±0.94 pA/pF and 1.49±0.70 pA/pF, respectively (n=6, p<0.05, Fig. 3C).

The H_2O_2-stimulated K_{Ca} currents were also decreased by

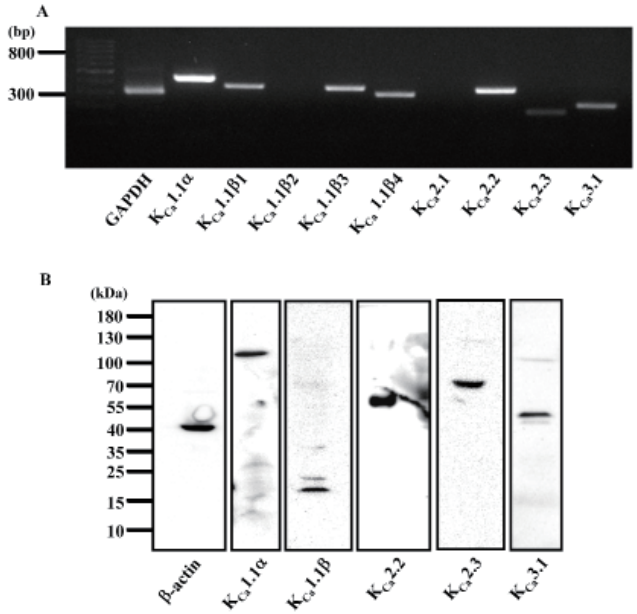

Fig. 2. Expression of various K_{Ca} channel subtypes in human cardiac fibroblasts. (A) RT-PCR showing strong mRNA expression of $K_{Ca}1.1α$, $K_{Ca}1.1β1$, $K_{Ca}1.1β3$, $K_{Ca}1.1β4$, and $K_{Ca}2.2$ and weak expression of $K_{Ca}2.3$ and $K_{Ca}3.1$. GAPDH was used as control. (B) Western blot analysis showing protein expression of $K_{Ca}1.1α$, $K_{Ca}1.1β$, $K_{Ca}2.2$, $K_{Ca}2.3$, and $K_{Ca}3.1$. β-actin was used as a loading control.

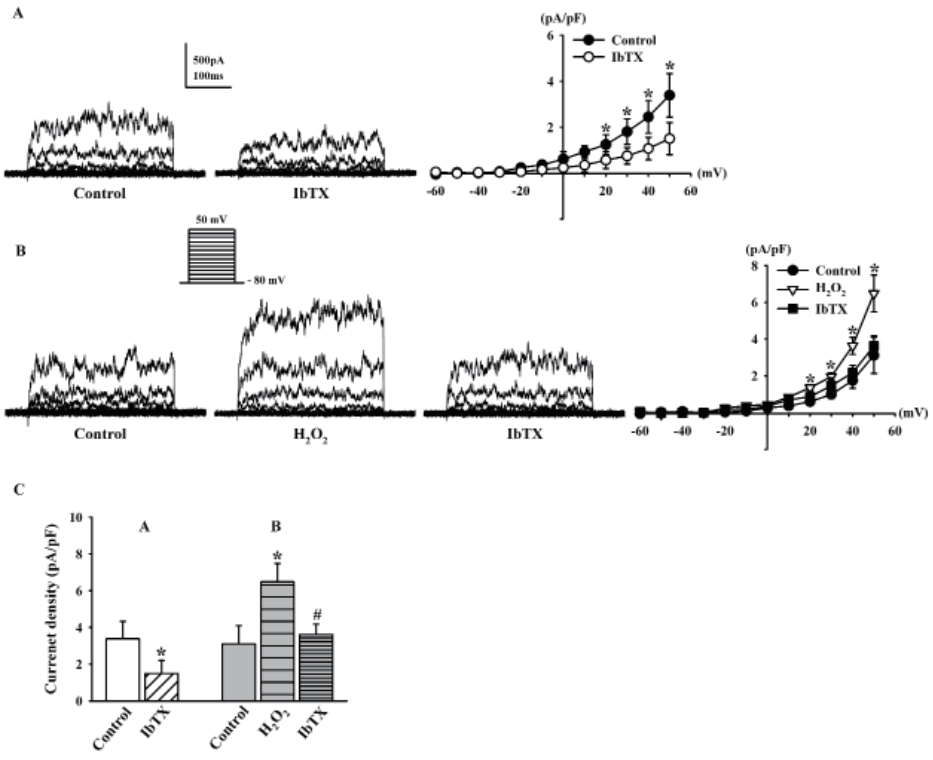

Fig. 3. Effect of iberiotoxin on outward K^+ currents and H_2O_2–activated K^+ currents in human cardiac fibroblasts. (A) Strongly oscillating K_{Ca} currents inhibited by100 nM IbTX. (B) Addition of 100 nM IbTX blocked the H_2O_2-activated K_{Ca} currents (C) Bar graph summarizing the effects of IbTX, and the effect of IbTX on K_{Ca} currents after pre-incubation with H_2O_2. *p<0.05, versus the control; #p<0.05, versus the H_2O_2.

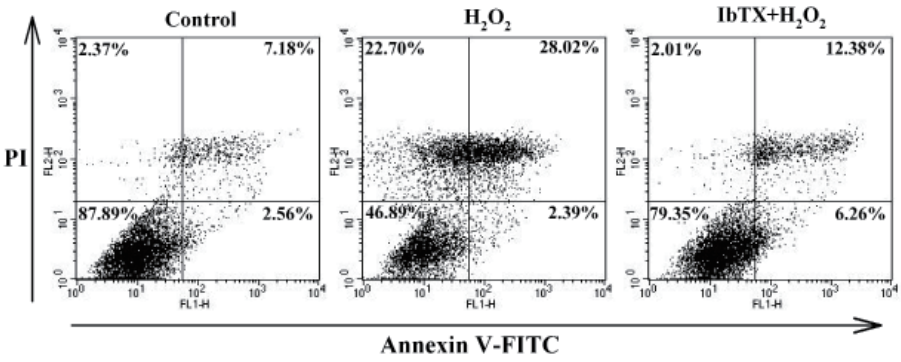

Fig. 4. Role of BK_{Ca} channels in H_2O_2-induced apoptosis. Monolayer of human cardiac fibroblasts was treated by 100 μM H_2O_2 for 24 h. The H_2O_2-induced apoptosis was inhibited in the presence of 100 nM IbTX. The cytogram of the flow cytometry analysis showing the percentages of cells with specific staining patterns; In the lower left-hand quadrant (annexin V negative, PI negative) are viable cells, in the lower right-hand quadrant (annexin V positive, PI negative) are early apoptotic cells, in the upper left-hand quadrant (annexin V negative, PI positive) are dead cells, and in the upper right-hand quadrant (annexin V positive, PI positive) are late apoptotic/necrotic cells.

IbTX (from 208.1±10.3% to 116.2±5.7%, n=5, *p<0.05 vs. control; Fig. 3B). The current densities of K_{Ca} currents at +50 mV in the control, H_2O_2, and IbTX were 3.11±0.98 pA/pF, 6.48±1.0 pA/pF, and 3.62±0.55 pA/pF, respectively (n=5, *p<0.05 vs. control, #p<0.05 vs. H_2O_2 ; Fig. 3C).

We next examined whether the H_2O_2-induced increase in BK_{Ca} currents was associated with H_2O_2-induced cell injury and found that IbTX attenuated the H_2O_2-induced apoptosis of HCFs. The apoptosis patterns of HCFs induced by H_2O_2 were analyzed by flow cytometry. The resulting cytogram shows the percentage of cells with an apoptosis-specific staining pattern (Fig. 4). In total, 28.02% of the cells treated with H_2O_2 showed late apoptotic changes, whereas 7.18% of control cells were late apoptotic. When we pretreated the cells with IbTX for 24 h before adding H_2O_2, only 12.38% of the cells showed the late apoptotic changes induced by H_2O_2. These data demonstrated that the inhibition of K^+ efflux through BK_{Ca} channels was able to inhibit late apoptosis and that H_2O_2-induced apoptotic cell death of HCFs is mediated by BK_{Ca} channels.

Signaling pathway for the effects of H_2O_2 on BK_{Ca} currents

We studied whether the effects of H_2O_2 on BK_{Ca} currents was

mediated by the cGMP signaling pathway. We added KT5823 (a PKG inhibitor, 1 μM) to the bath solution for 20 min, and then treated the cells with 100 μM H_2O_2. Under these conditions, H_2O_2 failed to increase BK_{Ca} currents (95.1±8.3%, n=7; Fig. 5A). When we pretreated the cells with ODQ (a soluble guanylate cyclase inhibitor, 10 μM) for 20 min, H_2O_2 also failed to increase BK_{Ca} currents (89.4±9.9%, n=5; Fig. 5B). We also assessed the effects of cGMP, which is generated by NO binding to soluble guanylate cyclase. Treatment with 8-Br-cGMP (a membrane-permeable cGMP analogue, 300 μM) increased the BK_{Ca} currents to 169.2±14.6% of the control at +50 mV (n=5, p<0.05 vs. control; Fig. 5C). Fig. 5D shows the effect of H_2O_2 on the current density at +50 mV after KT5823 pretreatment (control, 3.20±0.89 pA/pF; +KT5823, 3.02±1.63 pA/pF; +H_2O_2, 3.04±1.57 pA/pF) and ODQ pretreatment (control, 3.07±1.22 pA/pF; +ODQ, 2.70±1.34 pA/pF; +H_2O_2, 2.74±1.21 pA/pF). The effect of 8-Br-cGMP on BK_{Ca} currents is also shown (from 3.78±0.84 pA/pF to 6.39±1.22 pA/pF, p<0.05).

To determine whether PKA is also involved in the effect of H_2O_2 on BK_{Ca} currents, we pretreated fibroblasts with KT5720 and H-89, well-known PKA inhibitors. KT5720 (1 μM) was added to the bath solution for 20 min, and then H_2O_2 (100 μM) was added. KT5720 increased BK_{Ca} currents (116.9±15.6% of the control at +50 mV, n=6, Fig. 6A); however, this difference was not significant. BK_{Ca} currents were still increased by 100 μM H_2O_2 in the presence of KT5720 (224.1±22.2%, n=6, p<0.01 vs. control; Fig. 6A). H-89 (1 μM) also increased BK_{Ca} currents, and the difference was significant (131.2±12.9%, n=5, p<0.05 vs. control; Fig. 6B). However, pretreatment with H-89 did not inhibit the stimulatory effect of H_2O_2 on BK_{Ca} currents because 100 μM H_2O_2 increased the BK_{Ca} currents (174.7±12.6% of the control at +50 mV). Fig. 6C shows the effects of H_2O_2 on the current density at +50 mV after KT5720 pretreatment (control, 3.21±0.31 pA/pF; +KT5720, 3.69±0.48 pA/pF; +H_2O_2, 7.21±0.66 pA/pF) and H-89 pretreatment (control, 3.35±0.41 pA/pF; +H-89, 4.56±0.41 pA/pF; +H_2O_2, 5.85±0.50 pA/pF).

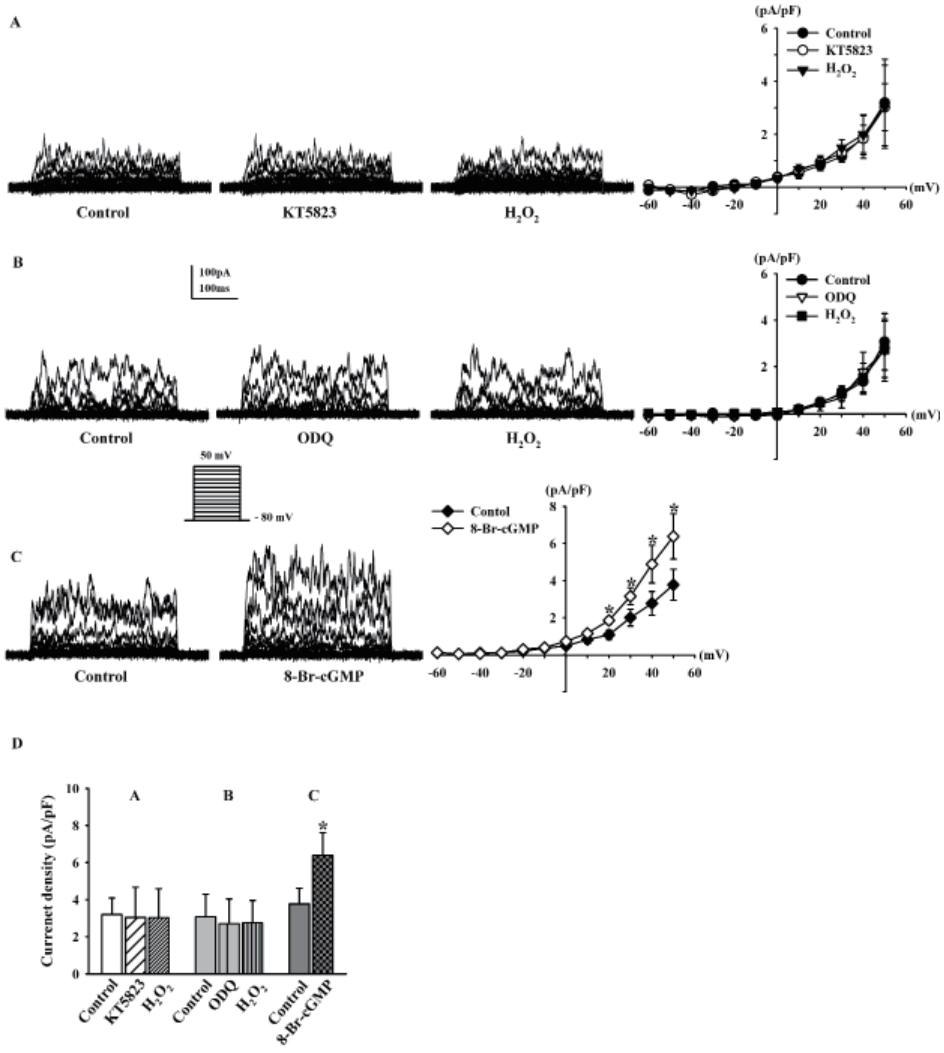

Fig. 5. Effects of PKG pathway modulation on H_2O_2-induced BK_{Ca} current changes. (A, B) Representative current traces showing the effect of 100 μM H_2O_2 on BK_{Ca} currents in the presence of 1 μM KT5823 and 1 μM ODQ. (C) Effect of 300 μM 8-Br-cGMP on BK_{Ca} currents. (D) Bar graph summarizing the effects of H_2O_2 on BK_{Ca} currents after pre-incubation with KT5823 or ODQ, and the effect of 8-Br-cGMP on BK_{Ca} currents. *p<0.05, versus the control.

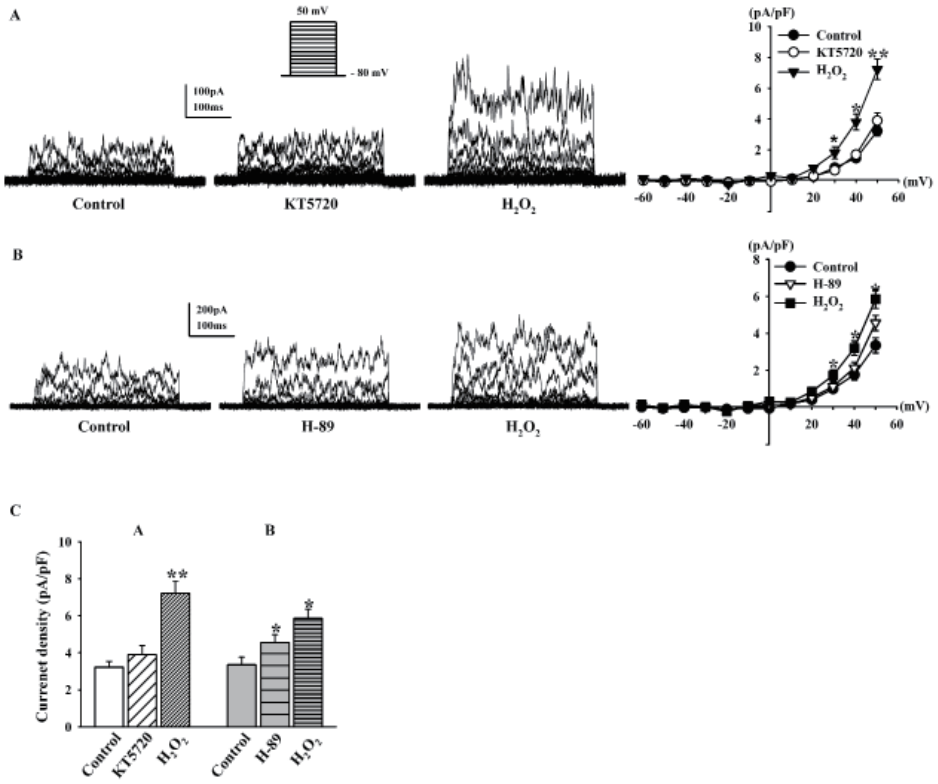

Fig. 6. Effects of PKA pathway modulation on H_2O_2-induced BK_{Ca} current changes. (A, B) Representative current traces showing the effect of 100 μM H_2O_2 on BK_{Ca} currents after pre-incubation with 1 μM KT5720 and 1 μM H-89. (C) Bar graph summarizing the effects of H_2O_2 on BK_{Ca} currents in the presence of KT5720 or H-89. *p<0.05, **p<0.01 versus the control.

DISCUSSION

The main finding of this study is that, among the VDKCs in HCFs, H_2O_2 stimulates BK_{Ca} currents but not K_{DR} or K_{TO} currents and that this H_2O_2-stimulating effect on BK_{Ca} currents is mediated by activation of protein kinase G (PKG) pathways but not the protein kinase A (PKA) pathway. In addition, H_2O_2-induced apoptosis of HCFs is mediated by BK_{Ca} channels.

The presence of VDKCs has been previously reported. These currents are thought regulate resting membrane potential, proliferation of ventricular fibroblasts [26], the functional expression of BK_{Ca} channels, and electrical coupling between cardiomyocytes and fibroblasts [25]. Li et al. [8] also reported the presence of three types of VDKCs in HCFs. However, we found some discrepancies between their results and ours. In their report, BK_{Ca} currents were present in most HCFs (88%), whereas K_{DR} and K_{TO} currents were present in a small population of cells (15 and 14%, respectively). In contrast, our results showed 47% of cells with K_{Ca} currents, 46.8% of cells with K_{DR} currents, and 6.2% of cells with K_{TO} currents. This difference may be due to some confusion in their report. We think that they may have miscounted K_{DR} currents as K_{Ca} currents. Their I-V curve of K_{Ca} currents did not show the strong outward rectification that is characteristic of K_{Ca} currents, even for currents inhibited by paxilline, this may explain why the K_{DR} current is co-present with the BK_{Ca} current in these cells. We also detected the coexistence of these three VDKCs in HCFs. To prevent confusion in identifying the types of K^+ current, we defined only strongly oscillating outward K^+ currents that had strong outward rectification in the I-V curve as K_{Ca} currents.

Furthermore, this earlier study [8] also showed significant mRNA expression of the $K_{Ca}1.1$ subunit of BK_{Ca} channels, but no mRNA expression of the 2.1 subunit of SK_{Ca} channels or the $K_{Ca}3.1$ subunit of IK_{Ca} was detected. In contrast, we detected mRNA expression of channel genes corresponding to the three subtypes of K_{Ca}, including clear mRNA amplification of the pore-forming α subunit of $K_{Ca}1.1$ (BK_{Ca}) channels and the auxiliary 1.1β1, 1.1β3, and 1.1β4 subunits, the $K_{Ca}2.2$ and $K_{Ca}2.3$ subunits of SK_{Ca} channels, and the $K_{Ca}3.1$ subunit of IK_{Ca} channels by RT-PCR. The protein expression of BK_{Ca}, SK_{Ca}, and IK_{Ca} channels ($K_{Ca}1.1$, $K_{Ca}2.2$, $K_{Ca}2.3$, and $K_{Ca}3.1$) was also detected as prominent bands in the western blot analysis. Even though these ion channels contribute to the electrical coupling between cardiomyocytes and fibroblasts, BK_{Ca} currents have not been detected in human cardiomyocytes [8,25].

In our experiment, the H_2O_2-increased, strongly oscillating, outward rectifying K_{Ca} currents were considered BK_{Ca} currents since they were inhibited by IbTX, a BK_{Ca}- specific channel blocker. In addition, these currents were activated by high Ca^{2+} levels introduced using an intra-pipette solution and a high-stimulation voltage, which is the cause of strong outward rectification.

Our results showing H_2O_2-enhanced BK_{Ca} currents in whole-cell recordings are consistent with previous reports on vascular

smooth muscle cells, human endothelial cells, and human dermal fibroblasts [9,22,27]. In contrast, in this study, H_2O_2 did not stimulate voltage-gated K^+ currents (K_{DR} and K_{TO} currents) in HCFs. These results are not consistent with previous studies in cardiomyocytes [23,24] and coronary vascular smooth muscle cells [28]. These differences in the distribution of K^+ currents and H_2O_2 effects imply variations in the functions of these channels in these two types of heart cells.

To the best of our knowledge, this is the first report showing that H_2O_2 enhances the BK_{Ca} currents of HCFs through PKG pathways but not through the PKA pathway. Several studies have reported that H_2O_2 stimulates BK_{Ca} channels through the PKG pathway in cultured human endothelial cells [22] and human coronary arterioles [29]. However, the effect of H_2O_2 on BK_{Ca} channels in HCFs and the underlying mechanism were not completely clear. In addition, inhibition of PKG by KT5823 and inhibition of soluble guanylate cyclase by ODQ attenuated the increase in BK_{Ca} currents following H_2O_2 exposure. 8-Br-cGMP, a membrane permeable analogue of cGMP, also increased BK_{Ca} currents. These results suggest that the PKG pathway is involved in the modulation of BK_{Ca} currents by H_2O_2 in HCFs.

Activation of BK_{Ca} channels likely elevates the intracellular Ca^{2+} level, which further enhances the release of NO in endothelial cells [30]. It has also been reported that NO increases BK_{Ca} currents in human dermal fibroblasts via the cGMP/PKG pathway [31] and cross-activation of the PKA pathway that stimulates currents through cGMP [32]. However, in this study, the H_2O_2-stimulating effects on BK_{Ca} currents were not decreased by pretreatment with KT5720 or H-89, suggesting that the PKA pathway is not involved in the modulation of BK_{Ca} currents by H_2O_2 in human cardiac fibroblasts. The stimulating effect of H-89 on BK_{Ca} currents was reported previously [33] and could explain the direct modulation of the currents observed here.

It is well known that K^+ channel-mediated signals play an important role in cell death or apoptosis and that increased K^+ efflux is one of the earliest indicators of apoptosis [10,12]. The K_{Ca} currents that are associated with apoptosis have been reported in a wide variety of cells [34,35]. When we pretreated cells with IbTX for 24 h before the addition of H_2O_2, the H_2O_2-induced early apoptotic changes decreased, which means that BK_{Ca} channels mediate early apoptotic cell death induced by H_2O_2 in HCFs. Similar results were also reported in human dermal fibroblasts [9]. We have also reported that activation of BK_{Ca} channels by its agonist, NS1619, mediates early apoptotic cell death in human dermal fibroblasts [36].

One limitation of the present study is that we cannot rule out the existence of other mechanisms for H_2O_2-induced cell injury in HCFs, especially the involvement of IK_{Ca} channels, since their expression was detected by RT-PCR and western blot analysis, and they also play important roles in cell proliferation [37,38].

ACKNOWLEDGEMENT

This work was supported by National Research Foundation of Korea Grant funded by the Korean Government (2010-0023712).

CONFLICTS OF INTEREST

The authors declare no conflicts of interest.

REFERENCES

1. Dixon IM, Cunnington RH. Mast cells and cardiac fibroblasts: accomplices in elevation of collagen synthesis in modulation of fibroblast phenotype. *Hypertension*. 2011;58:142-144.
2. Camelliti P, Borg TK, Kohl P. Structural and functional characterisation of cardiac fibroblasts. *Cardiovasc Res*. 2005;65:40-51.
3. Krenning G, Zeisberg EM, Kalluri R. The origin of fibroblasts and mechanism of cardiac fibrosis. *J Cell Physiol*. 2010;225:631-637.
4. Brown RD, Ambler SK, Mitchell MD, Long CS. The cardiac fibroblast: therapeutic target in myocardial remodeling and failure. *Annu Rev Pharmacol Toxicol*. 2005;45:657-687.
5. Flack EC, Lindsey ML, Squires CE, Kaplan BS, Stroud RE, Clark LL, Escobar PG, Yarbrough WM, Spinale FG. Alterations in cultured myocardial fibroblast function following the development of left ventricular failure. *J Mol Cell Cardiol*. 2006;40:474-483.
6. Kohl P, Camelliti P. Cardiac myocyte-nonmyocyte electrotonic coupling: implications for ventricular arrhythmogenesis. *Heart Rhythm*. 2007;4:233-235.
7. Kohl P, Camelliti P, Burton FL, Smith GL. Electrical coupling of fibroblasts and myocytes: relevance for cardiac propagation. *J Electrocardiol*. 2005;38(4 Suppl):45-50.
8. Li GR, Sun HY, Chen JB, Zhou Y, Tse HF, Lau CP. Characterization of multiple ion channels in cultured human cardiac fibroblasts. *PLoS One*. 2009;4:e7307.
9. Feng B, Ye WL, Ma LJ, Fang Y, Mei YA, Wei SM. Hydrogen peroxide enhanced Ca^{2+}-activated BK currents and promoted cell injury in human dermal fibroblasts. *Life Sci*. 2012;90:424-431.
10. Jiao S, Wu MM, Hu CL, Zhang ZH, Mei YA. Melatonin receptor agonist 2-iodomelatonin prevents apoptosis of cerebellar granule neurons via K^+ current inhibition. *J Pineal Res*. 2004;36:109-116.
11. Wu CT, Qi XY, Huang H, Naud P, Dawson K, Yeh YH, Harada M, Kuo CT, Nattel S. Disease and region-related cardiac fibroblast potassium current variations and potential functional significance. *Cardiovasc Res*. 2014;102:487-496.
12. Yu SP, Yeh CH, Sensi SL, Gwag BJ, Canzoniero LM, Farhangrazi ZS, Ying HS, Tian M, Dugan LL, Choi DW. Mediation of neuronal apoptosis by enhancement of outward potassium current. *Science*. 1997;278:114-117.
13. Yue L, Xie J, Nattel S. Molecular determinants of cardiac fibroblast electrical function and therapeutic implications for atrial fibrillation. *Cardiovasc Res*. 2011;89:744-753.
14. Toro L, Wallner M, Meera P, Tanaka Y. Maxi-K_{Ca}, a unique member of the voltage-gated K channel superfamily. *News Physiol Sci*.

1998;13:112-117.
15. Hoffman JF, Joiner W, Nehrke K, Potapova O, Foye K, Wickrema A. The hSK4 (KCNN4) isoform is the Ca^{2+}-activated K^+ channel (Gardos channel) in human red blood cells. *Proc Natl Acad Sci U S A*. 2003;100:7366-7371.
16. Ouadid-Ahidouch H, Roudbaraki M, Delcourt P, Ahidouch A, Joury N, Prevarskaya N. Functional and molecular identification of intermediate-conductance Ca^{2+}-activated K^+ channels in breast cancer cells: association with cell cycle progression. *Am J Physiol Cell Physiol.* 2004;287:C125-134.
17. Sheng JZ, Braun AP. Small- and intermediate-conductance Ca^{2+}-activated K^+ channels directly control agonist-evoked nitric oxide synthesis in human vascular endothelial cells. *Am J Physiol Cell Physiol.* 2007;293:C458-467.
18. Mathie A, Wooltorton JR, Watkins CS. Voltage-activated potassium channels in mammalian neurons and their block by novel pharmacological agents. *Gen Pharmacol.* 1998;30:13-24.
19. Park WS, Firth AL, Han J, Ko EA. Patho-, physiological roles of voltage-dependent K^+ channels in pulmonary arterial smooth muscle cells. *J Smooth Muscle Res.* 2010;46:89-105.
20. Sun Y. Myocardial repair/remodelling following infarction: roles of local factors. *Cardiovasc Res.* 2009;81:482-490.
21. Angelova P, Muller W. Oxidative modulation of the transient potassium current IA by intracellular arachidonic acid in rat CA1 pyramidal neurons. *Eur J Neurosci.* 2006;23:2375-2384.
22. Dong DL, Yue P, Yang BF, Wang WH. Hydrogen peroxide stimulates the Ca^{2+}-activated big-conductance K channels (BK) through cGMP signaling pathway in cultured human endothelial cells. *Cell Physiol Biochem.* 2008;22:119-126.
23. Dong DL, Liu Y, Zhou YH, Song WH, Wang H, Yang BF. Decreases of voltage-dependent K^+ currents densities in ventricular myocytes of guinea pigs by chronic oxidant stress. *Acta Pharmacol Sin.* 2004;25:751-755.
24. Huang SY, Lu YY, Chen YC, Chen WT, Lin YK, Chen SA, Chen YJ. Hydrogen peroxide modulates electrophysiological characteristics of left atrial myocytes. *Acta Cardiol Sin.* 2014;30:38-45.
25. Wang YJ, Sung RJ, Lin MW, Wu SN. Contribution of BK_{Ca}-channel activity in human cardiac fibroblasts to electrical coupling of cardiomyocytes-fibroblasts. *J Membr Biol.* 2006;213:175-185.
26. Chilton L, Ohya S, Freed D, George E, Drobic V, Shibukawa Y, Maccannell KA, Imaizumi Y, Clark RB, Dixon IM, Giles WR. K^+ currents regulate the resting membrane potential, proliferation, and contractile responses in ventricular fibroblasts and myofibroblasts. *Am J Physiol Heart Circ Physiol*. 2005;288:H2931-2939.
27. Brzezinska AK, Gebremedhin D, Chilian WM, Kalyanaraman B, Elliott SJ. Peroxynitrite reversibly inhibits Ca^{2+}-activated K^+ channels in rat cerebral artery smooth muscle cells. *Am J Physiol Heart Circ Physiol.* 2000;278:H1883-1890.
28. Rogers PA, Chilian WM, Bratz IN, Bryan RM Jr, Dick GM. H_2O_2 activates redox- and 4-aminopyridine-sensitive Kv channels in coronary vascular smooth muscle. *Am J Physiol Heart Circ Physiol.* 2007;292:H1404-1411.
29. Zhang DX, Borbouse L, Gebremedhin D, Mendoza SA, Zinkevich NS, Li R, Gutterman DD. H_2O_2-induced dilation in human coronary arterioles: role of protein kinase G dimerization and large-conductance Ca^{2+}-activated K^+ channel activation. *Circ Res.* 2012;110:471-480.
30. Matoba T, Shimokawa H, Nakashima M, Hirakawa Y, Mukai Y, Hirano K, Kanaide H, Takeshita A. Hydrogen peroxide is an endothelium-derived hyperpolarizing factor in mice. *J Clin Invest.* 2000;106:1521-1530.
31. Lim I, Yun J, Kim S, Lee C, Seo S, Kim T, Bang H. Nitric oxide stimulates a large-conductance Ca-activated K^+ channel in human skin fibroblasts through protein kinase G pathway. *Skin Pharmacol Physiol.* 2005;18:279-287.
32. Roh S, Choi S, Lim I. Involvement of protein kinase A in nitric oxide stimulating effect on a BK_{Ca} channel of human dermal fibroblasts. *J Invest Dermatol*. 2007;127:2533-2538.
33. Park WS, Son YK, Kim N, Youm JB, Warda M, Ko JH, Ko EA, Kang SH, Kim E, Earm YE, Han J. Direct modulation of Ca^{2+}-activated K^+ current by H-89 in rabbit coronary arterial smooth muscle cells. *Vascul Pharmacol.* 2007;46:105-113.
34. Krick S, Platoshyn O, Sweeney M, McDaniel SS, Zhang S, Rubin LJ, Yuan JX. Nitric oxide induces apoptosis by activating K^+ channels in pulmonary vascular smooth muscle cells. *Am J Physiol Heart Circ Physiol.* 2002;282:H184-193.
35. Ma YG, Dong L, Ye XL, Deng CL, Cheng JH, Liu WC, Ma J, Chang YM, Xie MJ. Activation of cloned BK_{Ca} channels in nitric oxide-induced apoptosis of HEK293 cells. *Apoptosis.* 2010;15:426-438.
36. Yun J, Park H, Ko JH, Lee W, Kim K, Kim T, Shin J, Kim K, Kim K, Song JH, Noh YH, Bang H, Lim I. Expression of Ca^{2+} -activated K^+ channels in human dermal fibroblasts and their roles in apoptosis. *Skin Pharmacol Physiol*. 2010;23:91-104.
37. Choi S, Lee W, Yun J, Seo J, Lim I. Expression of Ca-activated K channels and their role in proliferation of rat cardiac fibroblasts. *Korean J Physiol Pharmacol*. 2008;12:51-58.
38. Wang LP, Wang Y, Zhao LM, Li GR, Deng XL. Angiotensin II upregulates $K_{Ca}3.1$ channels and stimulates cell proliferation in rat cardiac fibroblasts. *Biochem Pharmacol.* 2013;85:1486-1494.